

Silver(I) and Thallium(I) Complexes of a PNP Ligand and Their Utility as PNP Transfer Reagents

Jessica C. DeMott,[†] Falguni Basuli,[‡] Uriah J. Kilgore,[‡] Bruce M. Foxman,[†] John C. Huffman,[‡] Oleg V. Ozerov,^{*,†} and Daniel J. Mindiola^{*,‡}

Department of Chemistry, Brandeis University, MS 015, 415 South Street, Waltham, Massachusetts 02454, and Department of Chemistry and Molecular Structure Center, Indiana University, Bloomington, Indiana 47405

Received January 13, 2007

Silver(I) and thallium(I) complexes of a diarylamido-based PNP pincer ligand have been prepared and characterized. The silver complex [(PNP)Ag]₂ exists as a dimer both in solution and in the solid state and is stable under an ambient atmosphere. Thallium complex (PNP)Tl is, however, monomeric and acutely sensitive to moisture and air. Both reagents serve to transfer PNP into the coordination sphere of divalent nickel, palladium, and platinum. [(PNP)-Ag]₂ is able to effect PNP transfer in air, but the transfer to nickel(II) is less efficient than that with the thallium(I) analogue.

Introduction

The diarylamido-based PNP ligands of the pincer family were first reported in 2003¹ and have given rise to some exciting transition-metal chemistry from a number of researchers, including both of our groups.^{2,3} Synthetic methods that allow convenient introduction of a ligand into the coordination sphere of the metal center are especially important for the installation of bulky anionic chelating ligands. Most commonly, anionic ligands are introduced via salt metathesis between a transition-metal chloride and a lithium or magnesium derivative of the incoming ligand. This has indeed been used in the chemistry of diarylamido-based

PNP ligands.^{1–3} The possibility of undesired side reactions stemming from the higher basicity and reducing power of lithium or magnesium derivatives may occasionally make derivatives of other metals be attractive for pincer ligand transfer purposes.⁴ Softer thallium(I) and silver(I) salts are frequently used to replace a halide on a transition-metal center with an anionic ligand. In this Article, we present the results of our investigation into the viability of silver and thallium PNP derivatives as PNP transfer agents as well as their structural characterization.

Results and Discussion

Synthesis and Structure of [(PNP)Ag]₂ (2). The preparation of (2) was accomplished by two different synthetic methods (Scheme 1). Vigorous stirring of (PNP)H (1) with Ag₂O in THF led to the formation of 2 (NMR spectroscopic evidence). This cleavage of the N–H bond by Ag₂O is reminiscent of the syntheses of silver complexes of N-heterocyclic carbenes (where Ag₂O cleaves a relatively acidic C–H bond).⁵ Alternatively, 2 could be prepared by mixing 1 with AgOAc in THF, followed by the addition of KOBu^t.

* To whom correspondence should be addressed. E-mail: ozerov@brandeis.edu (O.V.O.), mindiola@indiana.edu (D.J.M.).

[†] Brandeis University.

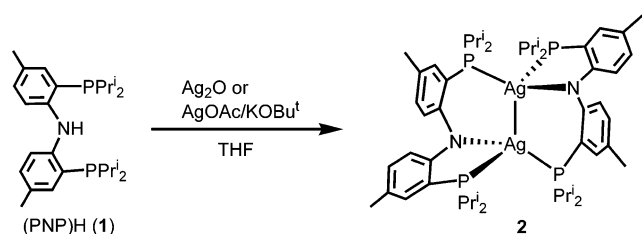
[‡] Indiana University.

- (1) (a) Liang, L.-C.; Lin, J.-M.; Hung, C.-H. *Organometallics* **2003**, *22*, 3007. (b) Winter, A. M.; Eichele, K.; Mack, H.-G.; Potuznik, S.; Mayer, H. A.; Kaska, W. C. *J. Organomet. Chem.* **2003**, *682*, 149. (c) Fan, L.; Foxman, B. M.; Ozerov, O. V. *Organometallics* **2004**, *23*, 326. (d) Liang, L.-C. *Coord. Chem. Rev.* **2006**, *250*, 1152.
- (2) (a) Mindiola, D. J. *Acc. Chem. Res.* **2006**, *39*, 813. (b) Kilgore, U. J.; Yang, X.; Tomaszewski, J.; Huffman, J. C.; Mindiola, D. J. *Inorg. Chem.* **2006**, *45*, 10712. (c) Bailey, B. C.; Fan, H.; Baum, E. W.; Huffman, J. C.; Baik, M.-H.; Mindiola, D. J. *J. Am. Chem. Soc.* **2005**, *127*, 16016. (d) Bailey, B. C.; Huffman, J. C.; Mindiola, D. J.; Weng, W.; Ozerov, O. V. *Organometallics* **2005**, *24*, 1390.
- (3) (a) Fafard, C. M.; Ozerov, O. V. *Inorg. Chim. Acta* **2007**, *360*, 286. (b) Gatard, S.; Çelenligil-Çetin, R.; Guo, C.; Foxman, B. M.; Ozerov, O. V. *J. Am. Chem. Soc.* **2006**, *128*, 2808. (c) Fan, L.; Parkin, S.; Ozerov, O. V. *J. Am. Chem. Soc.* **2005**, *127*, 16772. (d) Weng, W.; Guo, C.; Çelenligil-Çetin, P. R.; Foxman, B. M.; Ozerov, O. V. *Chem. Commun.* **2006**, 197.

(4) Contel, M.; Stol, M.; Casado, M. A.; Van Klink, G. P. M.; Ellis, D. D.; Spek, A. L.; Van Koten, G. *Organometallics* **2002**, *21*, 4556.

(5) (a) Wang, H. M. J.; Lin, I. J. B. *Organometallics*, **1998**, *17*, 972. (b) Simons, R. S.; Custer, P.; Tessier, C. A.; Youngs, W. J. *Organometallics* **2003**, *22*, 1979. (c) Hu, X.; Castro-Rodriguez, I.; Olsen, K.; Meyer, K. *Organometallics* **2004**, *23*, 755. (d) De Fremont, P.; Scott, N. M.; Stevens, E. D.; Ramnial, T.; Lightbody, O. C.; Macdonald, C. L. B.; Clyburne, J. A. C.; Abernethy, C. D.; Nolan, S. P. *Organometallics* **2005**, *24*, 6301.

Scheme 1



Solution NMR spectroscopic data for **2** at 22 °C are consistent with a time-averaged C_2 or C_s symmetry. A single, somewhat broadened, $^{31}\text{P}\{^1\text{H}\}$ NMR resonance was detected, displaying the two-douplets pattern typical of the coupling to two $S = 1/2$ isotopes of silver (^{107}Ag and ^{109}Ag ; $J^{107}\text{Ag-P} = 449$ Hz, $J^{109}\text{Ag-P} = 398$ Hz in C_6D_6). Two resonances were observed for the methine protons of the ^iPr groups, and four doublet-of-douplets resonances were observed for the ^iPr methyl groups. A closely related “[$(\text{C}_2\text{PCH}_2\text{SiMe}_2)_2\text{N}\text{Ag}$ ” (**3**) containing a disilylamido-based PNP ligand was reported (but not structurally characterized) by Caulton et al.⁶ The $J^{109}\text{Ag-P} = 500$ Hz in **3** is somewhat larger than that in **2**, likely a consequence of the greater donicity of the trialkylphosphine arms in **3** versus the aryladialkylphosphine arms in **2**.

An X-ray diffraction study on a crystal of **2** revealed a dimeric structure in the solid state (Figure 1). The structure contains a close $\text{Ag}^{\text{I}}-\text{Ag}^{\text{I}}$ contact of ca. 3.07 Å. The nature of closed-shell $d^{10}-d^{10}$ interactions was reviewed elsewhere; the $\text{Ag}-\text{Ag}$ distance in **2** is comparable to those of other examples of $\text{Ag}^{\text{I}}-\text{Ag}^{\text{I}}$ interactions.⁷ Each Ag center in **2** is bound to an amido donor and to two phosphine donors (one from each PNP unit). Two other structurally characterized dimeric complexes of a general formula $[(\text{PNP})\text{M}]_2$ have been reported: $[(\text{PNP})\text{Cu}]_2$ (**4**) of Peters and Harkins⁸ and $[(\text{PNP})\text{Co}]_2$ (**5**) of Mindiola et al.⁹ Both **4** and **5** adopt a diamond-shaped N_2M_2 structure in which the two amido ligands are bridging; this is not the case for **2**. The structure of **2** can be derived from those of **4** and **5** by scission of a pair of bridging $\text{M}-\text{N}$ bonds (resulting in two terminal amido ligands) and can thus be viewed as a dimer in which the two “halves” are associated somewhat less tightly. The $\text{Ag}-\text{Ag}$ distance in **2** is considerably larger than the $\text{M}-\text{M}$ distances in **4** (ca. 2.62 Å) and **5** (ca. 2.25 Å). The $\text{Ag}-\text{P}$ and $\text{Ag}-\text{N}$ distances in **2** are also considerably greater than the corresponding $\text{Cu}-\text{N}$ and $\text{Cu}-\text{P}$ distances in **4**.⁸ It is likely that the larger size of Ag , compared with the first-row metals Cu and Co , disfavors bridging. In addition, the phosphines in **4** bear smaller ^iBu substituents,⁸ and the larger PPr^i_2 arms in **2** may contribute to the formation of a more loosely associated dimeric structure. In **5**, the stronger bonding between the two d^8 Co^{I} centers accounts for a much shorter $\text{Co}-\text{Co}$ distance.⁹ One of the four $\text{P}-\text{C}-\text{C}-\text{N}$ dihedrals in the structure of **2** deviates significantly from

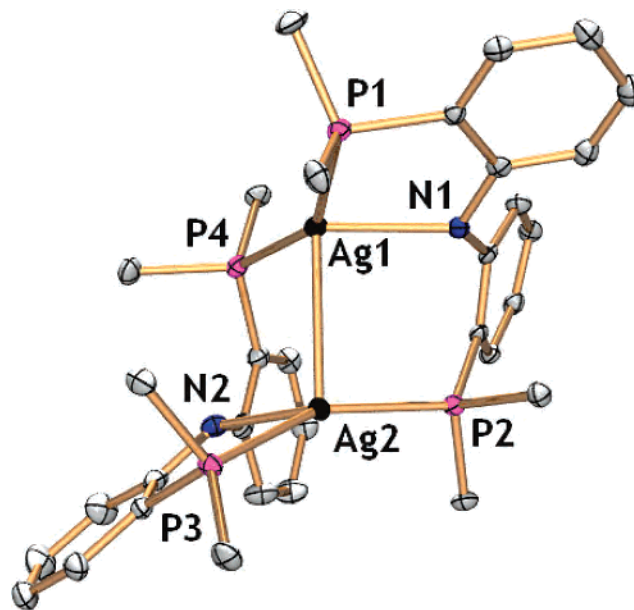


Figure 1. ORTEP¹² drawing (50% probability ellipsoids) of **2** showing selected atom labeling. H atoms and all of the methyl groups are omitted for clarity. Selected bond distances (Å) and angles (deg) follow: $\text{Ag1}-\text{Ag2}$, 3.0738(3); $\text{Ag1}-\text{P1}$, 2.4466(8); $\text{Ag1}-\text{P4}$, 2.4051(8); $\text{Ag2}-\text{P2}$, 2.3808(8); $\text{Ag2}-\text{P3}$, 2.4370(8); $\text{Ag1}-\text{N1}$, 2.340(2); $\text{Ag2}-\text{N2}$, 2.280(2); $\text{P1}-\text{Ag1}-\text{P4}$, 149.34(3); $\text{P2}-\text{Ag2}-\text{P3}$, 151.58(3); $\text{P1}-\text{Ag1}-\text{N1}$, 77.73(6); $\text{P4}-\text{Ag1}-\text{N1}$, 128.94(6); $\text{P2}-\text{Ag2}-\text{N2}$, 119.60(6); $\text{P3}-\text{Ag2}-\text{N2}$, 79.73(6); $\text{Ag2}-\text{Ag1}-\text{P1}$, 111.60(2); $\text{Ag2}-\text{Ag1}-\text{P4}$, 87.29(2); $\text{Ag1}-\text{Ag2}-\text{P2}$, 85.24(2); $\text{Ag1}-\text{Ag2}-\text{P3}$, 117.73(2); $\text{Ag2}-\text{Ag1}-\text{N1}$, 87.16(6); $\text{Ag1}-\text{Ag2}-\text{N2}$, 88.81(6).

planarity (ca. 15°; others are less than 5°), indicating that the structure of **2** is somewhat strained.

The $\text{Ag}-\text{N}_{\text{amido}}$ distances in **2** (ca. 2.28 and 2.34 Å) are longer than those in $[(\mu-(\text{Me}_3\text{Si})_2\text{N})\text{Ag}]_4$ (**6**; ca. 2.15 Å)¹⁰ and in the polymeric $[(\text{MeSO}_2)_2\text{N})\text{Ag}(m\text{-pyrazine})(\text{NCMe})]_{\infty}$ (**7**; ca. 2.24 Å).¹¹ This is rather surprising given the bridging nature of the amido ligands in **6** and that the dimesylamido ligand in **7** is more weakly donating than the diarylamido ligand in **2**.

We resorted to low-temperature NMR studies to probe whether the dimeric structure of **2** persists in solution. A $^{31}\text{P}\{^1\text{H}\}$ NMR spectrum of **2** collected at -70 °C in CD_2Cl_2 contained two ^{31}P NMR resonances, consistent with the nonequivalence of two phosphine arms with each PNP ligand in the solid-state structure of **2**. Each of the -70 °C $^{31}\text{P}\{^1\text{H}\}$ NMR resonances appeared as a broadened doublet. Presumably, the broadening precludes the resolution of two concentric doublets that ought to be observed from coupling to the two isotopes of silver (^{107}Ag , 51.8%; ^{109}Ag , 48.2%). The broadening probably arises from a fluxional process involving the PNP ligand and possibly also from weak spin-spin coupling between inequivalent ^{31}P nuclei. Thus, it appears that the solid-state structure is preserved in solution (at least, as the ground state at low temperature). At 22 °C, a fluxional process must effect the equilibration of the phosphorus environments rapidly on the NMR time scale.

(6) Ozerov, O. V.; Gerard, H. F.; Watson, L. A.; Huffman, J. C.; Caulton, K. G. *Inorg. Chem.* **2002**, *41*, 5615.

(7) Pyykko, P. *Chem. Rev.* **1997**, *97*, 597.

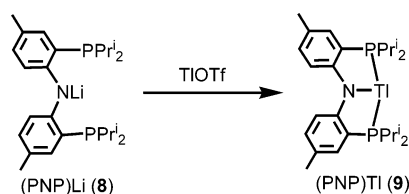
(8) Harkins, S. B.; Peters, J. C. *J. Am. Chem. Soc.* **2005**, *127*, 2030.

(9) Fout, A. R.; Basuli, F.; Fan, H.; Tomaszewski, J.; Huffman, J. C.; Baik, M.-H.; Mindiola, D. J. *Angew. Chem., Int. Ed.* **2006**, *45*, 3291.

(10) Hitchcock, P. B.; Lappert, M. F.; Pierssens, L. J.-M. *Chem. Commun.* **1996**, 1189.

(11) Lange, I.; Jones, P. G.; Blaschette, A. Z. *Anorg. Allg. Chem.* **1995**, *621*, 476.

Scheme 2



Notably, the average of the two apparent (ca. 445 Hz, presumably the approximate average of $J^{107}\text{Ag-P}$ and $J^{109}\text{Ag-P}$) $J_{\text{Ag-P}}$ coupling constants at $-70\text{ }^{\circ}\text{C}$ is equal, within the substantial error of measurement arising from the broadness of the peaks, to the average of the $J^{107}\text{Ag-P}$ and $J^{109}\text{Ag-P}$ coupling constants of the single resonance observed at $22\text{ }^{\circ}\text{C}$ (435 Hz in CD_2Cl_2). It is possible that the process responsible for the exchange of ^{31}P nuclei involves dissociation of dimeric **2** into monomeric (PNP)Ag species and subsequent recombination. However, a concerted intramolecular process in **2** cannot be ruled out.

Synthesis and Structure of (PNP)TI (9). When a THF solution of TIOTf was slowly added to a THF solution containing (PNP)Li (**8**), (PNP)TI (**9**) was isolated as an orange powder in 82% yield upon workup (Scheme 2). As expected for a thallium(I) reagent, **9** is diamagnetic and displays a C_{2v} symmetric system in the ^1H NMR spectrum at $22\text{ }^{\circ}\text{C}$. A single phosphorus resonance (δ , 48.33) was found in the $^{31}\text{P}\{^1\text{H}\}$ NMR spectrum with a significant $J_{\text{P-Tl}}$ coupling of 2385 Hz (^{203}Tl , $I = 1/2$, 29.5%; ^{205}Tl , $I = 1/2$, 70.5%). Conversely, we were able to obtain the $^{203/205}\text{Tl}$ NMR data for **9** and locate a triplet at 3229 ppm with a similar $J_{\text{Tl-P}}$ of ~ 2400 Hz. These coupling constants are lower than those observed by Peters et al. for $\text{Tl}[\text{PhBP}_3]$ (> 5000 Hz, $\text{PhBP}_3 = \text{Ph}(\text{CH}_2\text{PR}_2)_3$, $\text{R} = \text{Ph}$, $^{13a}\text{ }^i\text{Pr}^{13b}$) and $\text{Tl}[\text{Ph}_2\text{B}(\text{CH}_2\text{-PPh}_2)_2]$ (> 4000 Hz)^{13c} but greater than those for the thallium(III) phosphine adducts $\text{Tl}(\text{C}_6\text{H}_4\text{CH}_2\text{PPh}_2)_3$,¹⁴ $\text{Tl}(\text{CH}_2\text{SiMe}_3)_3\text{-P}[\text{SiMe}_3]_3$,¹⁵ and $[\text{Tl}(\text{CH}_3)_2(\mu_2\text{-P}[\text{SiMe}_3]_2)]_2$.¹⁶ In fact, **9** represents a rare example of a thallium(I) phosphine adduct, which is surprising given the assumption that a soft thallium(I) should readily coordinate soft donors such as a phosphine.¹⁷

To elucidate the degree of aggregation in **9** and to establish the coordination sphere about the Tl^{I} ion, we collected X-ray

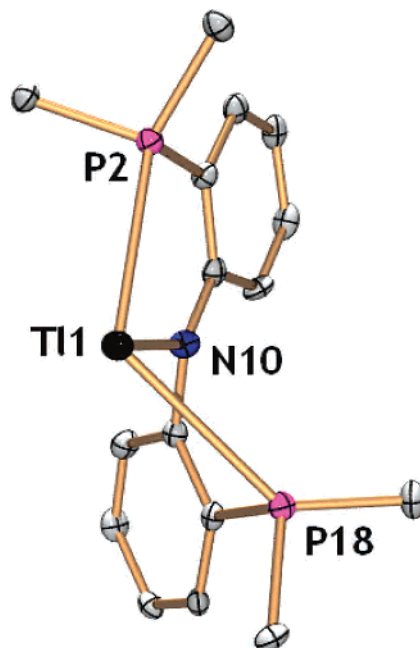


Figure 2. ORTEP¹² drawing (50% probability ellipsoids) of **9** showing selected atom labeling. H atoms and all of the methyl groups are omitted for clarity. Selected bond distances (Å) and angles (deg) follow: Tl1–N10, 2.413(3); Tl1–P2, 2.9708(9); Tl1–P18, 3.1076(10); N10–Tl1–P2, 68.00(7); N10–Tl1–P18, 64.88(7); P2–Tl1–P18, 118.81(2).

diffraction data on a single orange crystal of **9** (Figure 2). The PNP ligand in **6** adopts a conformation that is similar to that of itself in (PNP)Li(THF)¹⁸ and also to that of the bis(quinoly)amido NNN ligand in (NNN)TI reported by Peters et al.¹⁹ The two aryl rings of PNP are strongly twisted out of coplanarity, and the P–Tl–P angle is reduced to ca. 119° . Distortion from an idealized T-shaped geometry can be illustrated by the significant displacement ($\sim 1.82\text{ Å}$) of one of the P atoms (P18) from the imaginary mean plane defined by the atoms Tl1, P2, and N10. This highly distorted arrangement of ligands about Tl is presumably a consequence of a compromise between the inherent backbone constraints of the PNP ligand and the desired trigonal-pyramidal geometry about Tl^{I} .^{13,20} Examination of the unit cell does not suggest any $\text{Tl}\cdots\text{Tl}$ interatomic contacts playing a role in the solid-state structure for **9**. Another salient feature in the molecular structure of **9** is the Tl–N distance of 2.413(3) Å, which is longer than the one-coordinate Tl^{I} –amide distances 2.348(3) and 2.379(3) Å reported in the literature²¹ or from the monomeric, three-coordinate $\text{Tl-N}_{\text{amide}}$ system $\text{Tl}(\text{L})$ ($\text{L}^- = \text{bis}(3,5\text{-di-}i\text{-tert-butylpyrazol-1-yl})\text{-1-CH}_2\text{NAr}$, $\text{Ar} = 2,6\text{-}i\text{-Pr}_2\text{C}_6\text{H}_3$) (2.274(4) Å).²² Regardless, the Tl–N_{amide}

(12) (a) ORTEP plots were created using Ortep-3 for Windows. Farugia, L. *J. Appl. Crystallogr.* **1997**, *30*, 565. (b) 3D rendering was done using Persistence of Vision Ray Tracer (POV-Ray), available at <http://www.povray.org/>.

(13) (a) Shapiro, I. R.; Jenkins, D. M.; Thomas, J. C.; Day, M. W.; Peters, J. C. *Chem. Commun.* **2001**, 2152. (b) Betley, T. A.; Peters, J. C. *Inorg. Chem.* **2003**, *42*, 5074. (c) Thomas, J. C.; Peters, J. C. *Inorg. Chem.* **2003**, *42*, 5055.

(14) Muller, G.; Lachmann, J. *Z. Naturforsch., B: Anorg. Chem.* **1993**, *48*, 1544.

(15) Baldwin, R. A. R.; Wells, L.; White, P. S. *Main Group Chem.* **1986**, *2*, 67.

(16) Thomas, F.; Schulz, S.; Mansikkamaki, H.; Nieger, M. *Angew. Chem., Int. Ed.* **2003**, *42*, 5641.

(17) (a) Janiak, C. *Coord. Chem. Rev.* **1997**, *163*, 107. (b) For a collection of Ag^{I} and Tl^{I} adducts, see: (c) Rasika Dias, H. V. In *Comprehensive Coordination Chemistry II*; McCleverty, J. A., Meyer, T. J., Eds.; Elsevier: London, U.K., 2004; Vol. 3, pp 383–463. (d) Gimeno, M. C.; Laguna, A. In *Comprehensive Coordination Chemistry II*; McCleverty, J. A., Meyer, T. J., Eds.; Elsevier: London, U.K., 2004; Vol. 6, pp 911–1145.

(18) Weng, W.; Yang, L.; Foxman, B. M.; Ozerov, O. V. *Organometallics* **2004**, *23*, 4700.

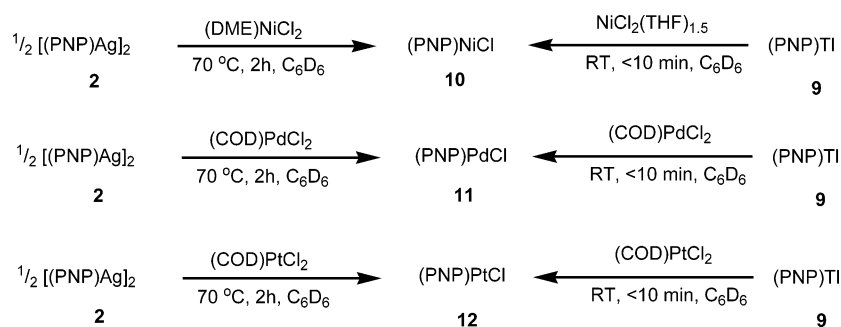
(19) Peters, J. C.; Harkins, S. B.; Brown, S. D.; Day, M. W. *Inorg. Chem.* **2001**, *40*, 5083.

(20) For some structurally characterized thallium(I) monomers bearing 3-*t*-Bu-substituted tris(pyrazolyl)borate ligands, see: (a) Ghosh, P.; Churchill, D. G.; Rubinshtein, M.; Parkin, G. *New J. Chem.* **1999**, *23*, 961. (b) Cowley, A. H.; Geerts, R. L.; Nunn, C. M.; Trofimenko, S. *J. Organomet. Chem.* **1989**, *365*, 19. (c) Yoon, K.; Parkin, G. *Polyhedron* **1995**, *14*, 811.

(21) Wright, R. J.; Brynda, M.; Power, P. P. *Inorg. Chem.* **2005**, *44*, 3368.

(22) Adhikari, D.; Zhao, G.; Basuli, F.; Tomaszewski, J.; Huffman, J. C.; Mindiola, D. J. *Inorg. Chem.* **2006**, *45*, 1604.

Scheme 3



distance in **1** is comparable to other Tl^I–amide distances reported in the literature.²³

Stability of **2 and **9**.** Complex **9** can be stored in the dark and at –35 °C without decomposition for approximately 2 weeks. It is recommended that the solid be used within a week of its preparation. However, gradual decomposition is eventually observed to deposit an intractable and insoluble black/gray material. We speculate that this dark product is the deposition of thallium metal. This complex is also thermally unstable and decomposes at temperatures over 140 °C (color change from orange to dark brown without melting). Solid **9** or its solutions must be handled under an inert atmosphere; otherwise, immediate decomposition ensues. These properties of **9** are in stark contrast to the Ag^I pincer analogue **2**, which is stable in ambient air both in solution and in the solid state for extended periods of time and shows no detectable sensitivity to ambient light. The resistance of **2** to hydrolysis is not surprising given that it can be synthesized from (PNP)H and Ag₂O (vide supra). In contrast to **2**, solutions of the parent ligand **1** degrade readily in air, which makes the former material an attractive reagent for subsequent transmetalation reactions.

Transmetalation Reactions. To test the viability of **2** and **9** as PNP transfer agents, we elected to explore their utility in the syntheses of (PNP)MCl complexes (**10–12**) of the metals of group 10 (Ni, Pd, Pt). The square-planar, diamagnetic (PNP)MCl complexes (**10–12**) were characterized previously and were shown to be exceedingly robust, including upon exposure to air.^{1c,24} We selected typical soluble adducts of the dichlorides of the corresponding metals (DME)NiCl₂, NiCl₂(THF)_{1.5}, (COD)PdCl₂, and (COD)PtCl₂ as PNP transfer recipients.

Reactions of **2** with L_nMCl₂ were performed in air, using commercial C₆D₆ that had not been dried or deoxygenated. In all three reactions, immediate changes were observed upon mixing. A temperature of 70 °C was maintained for 2 h to ensure completeness of the reactions. In the reactions with (COD)PdCl₂ and (COD)PtCl₂, 90% conversion to the products (**11** and **12**) was detected by NMR spectroscopy. The reaction with (DME)NiCl₂ proceeded less smoothly. Whereas substantial quantities of (PNP)NiCl (**10**) were produced, a mixture of apparently paramagnetic compounds

(broad, featureless resonances in the ¹H NMR spectrum) was also formed. The overlap among the peaks did not allow for the quantification of produced **10**. It is possible that the lesser affinity of Ni^{II} for phosphine donors results in an incomplete transfer of PNP and an observable equilibrium where Ag^I and Ni^{II} compete for binding to PNP. Alternatively, the oxidizing ability of Ag^I might interfere with clean salt metathesis.

In view of the sensitivity of **9** to air and moisture, the PNP transfer reactions with it were performed under an inert atmosphere in dried and degassed C₆D₆. Complex **9** served well to transfer PNP to Ni^{II}, Pd^{II}, and Pt^{II} in 85% or greater conversion (NMR spectroscopic evidence). In contrast to the reactivity of **2**, the reactions using **9** were essentially complete in the time of mixing.

Thus, in terms of PNP transfer, **9** behaves similarly to (PNP)Li,^{1–3} with fast PNP transfer but with sensitivity to moisture and air. **2** presents itself as a more sluggish (possibly owing to its dimeric nature) but robust PNP transfer agent. The two properties are probably related. It is reasonable to expect Ag^I to form stronger bonds to phosphines, thus preventing their oxidation and disfavoring Ag–N bond hydrolysis by holding Ag firmly in place. However, the stronger Ag–P bonds may result in (a) a more sluggish PNP transfer (for instance, if phosphine dissociation is involved in the rate-limiting step) and (b) a lack of thermodynamic driving force for a full PNP transfer to a metal with lesser phosphine affinity, such as Ni^{II}. It is also likely that the oxidizing nature of Ag(I) in **2** may lead to side reactions.

Conclusion

In summary, we have prepared and fully characterized silver(I) and thallium(I) derivatives of a diarylamido-based PNP ligand and investigated their stability and reactivity in the transmetalation reactions. The thallium derivative (PNP)Tl (**9**) exists as a monomer and behaves similarly to (PNP)Li in that it is sensitive to air and moisture (and possibly light sensitive) and rapidly transfers the anionic PNP ligand to divalent nickel, palladium, and platinum. The silver derivative [(PNP)Ag]₂ (**2**) exists as a dimer both in the solid state and in solution and is stable to air and moisture. It works well to transfer PNP to divalent palladium and platinum, but does so slowly. These results provide helpful insight for designing syntheses of transition-metal complexes of the PNP ligands and possibly those of other pincer ligands as well.

(23) For a review on thallium(I) amides, see: Gade, L. H. *Dalton Trans.* **2003**, 267.

(24) Ozerov, O. V.; Guo, C.; Fan, L.; Foxman, B. M. *Organometallics* **2004**, *23*, 5573.

Experimental Section

General Considerations. Unless specified otherwise, all of the manipulations were performed under an argon or nitrogen atmosphere using standard Schlenk-line or glovebox techniques. Toluene, pentane, Et₂O, C₆D₆, and THF and isooctane were dried over NaK/Ph₂CO/18-crown-6, distilled or vacuum-transferred and stored over molecular sieves in a glovebox under argon or nitrogen. Alternatively, anhydrous *n*-hexane, pentane, toluene, and benzene were purchased from Aldrich in sure-sealed reservoirs (18 L) and dried by passage through two columns of activated alumina and a Q-5 column,²⁵ whereas Et₂O and CH₂Cl₂ were dried by passage through two columns of activated alumina.²⁶ CD₂Cl₂ was dried over and vacuum-transferred from CaH₂. Celite, alumina, and 4 Å molecular sieves were activated under a vacuum overnight at 200 °C. (PNP)-Li (**8**),¹⁸ TlOTf,²⁷ NiCl₂(THF)_{1.5},²⁸ (DME)NiCl₂,²⁹ (COD)PdCl₂,³⁰ and (COD)PtCl₂³⁰ were prepared according to the literature. (PNP)-NiCl (**10**),²⁴ (PNP)PdCl (**11**),^{1c} and (PNP)PtCl (**12**)²⁴ were characterized elsewhere. All of the other chemicals were used as received from commercial vendors. NMR spectra were recorded on a Varian Inova 400 (¹H NMR, 399.755 MHz; ¹³C NMR, 100.518 MHz; ³¹P NMR, 161.822 MHz) spectrometer. For ¹H and ¹³C NMR spectra, the residual solvent peak was used as an internal reference. ³¹P NMR spectra were referenced externally using 85% H₃PO₄ at 0 ppm. Elemental analyses were performed by CALI Labs, Inc. (Parsippany, NJ) or Desert Analytics, (Tucson, AZ). ¹H, ³¹P, and ¹³C NMR spectra were recorded on Varian 400 or 300 MHz NMR spectrometers. ¹H and ¹³C NMR spectra are reported with reference to solvent resonances; ³¹P NMR spectra were referenced externally to 85% H₃PO₄ (Wilmad) at 0 ppm. ²⁰⁵Tl NMR spectral data were collected on a Varian Inova 500 instrument. Chemical shifts were externally referenced to 0.1 M aqueous Tl(NO₃) at 0.0 ppm. Spectra were recorded using 16 scans with a 45° pulse width over a spectral window of 1728 ppm. The acquisition time was 0.524 s, and the relaxation delay was 5 s.

[(PNP)Ag]₂ (2). Method 1. In a 10 mL Schlenk flask covered with foil, (PNP)H (**1**) (25.3 mg, 0.0592 mmol) was dissolved in THF. Ag₂O (8.4 mg, 0.0362 mmol) was added, and the solution was stirred for approximately 48 h. The formation of **2** was confirmed in situ by ³¹P{¹H} NMR. **Method 2.** In a Schlenk flask covered with foil, **1** (261 mg, 0.606 mmol) was dissolved in THF. AgOAc (103 mg, 0.681 mmol) was added, followed by the addition of KOBu^t (85.5 mg, 0.762 mmol). The solution was stirred for 3 h and then filtered through a pad of Celite and silica gel. The volatiles were removed from the filtrate, some pentane was added, and the flask was placed in a freezer at -35 °C overnight. The next day, the yellow solid was collected and dried under a vacuum (211 mg). A second fraction of 30 mg was obtained from the supernatant, for a total yield of 241 mg (74%). A C₆D₆ sample solution was left open to the air for 7 days without measurable degradation as assessed by NMR. No data were collected beyond 7 days. ¹H NMR (22 °C, C₆D₆): δ 7.14 (d, 2H, *J* = 7 Hz, Ar-*H*), 6.92 (d, 2H, *J* = 8 Hz, Ar-*H*), 6.86 (s, 2H, Ar-*H*), 2.49 (br s, 2H, CH(CH₃)₂), 2.25 (s, 6H, CH₃-Ar), 2.11 (br s, 2H, CH(CH₃)₂), 1.25 (dd, 6H, *J* = 14 and 7 Hz, CH(CH₃)₂), 1.14 (dd, 6H, *J* = 17 and 11 Hz, CH-

(CH₃)₂), 1.05 (dd, 6H, *J* = 13 and 7 Hz, CH(CH₃)₂), 1.00 (dd, 6H, *J* = 14 and 7 Hz, CH(CH₃)₂). ¹H NMR (22 °C, CD₂Cl₂): δ 6.72 overlapping with 6.69 (both s, 6H, Ar-*H*), 2.51 (br s, 2H, PCHMe₂), 2.14 (s, appears to be overlapping with a broad singlet, 6H, Ar-CH₃, with, 2H, PCHMe₂), 1.20 (dd, 6H, *J* = 15 and 8 Hz), 1.12 (dd, 6H, *J* = 15 and 8 Hz), 1.05 (dd, 6H, *J* = 14 and 7 Hz), 0.95 (dd, 6H, *J* = 14 and 7 Hz). ³¹P{¹H} NMR (CD₂Cl₂): δ 9.64 (d, *J*_{Ag-P} = 411 Hz, *J*_{109-P} = 459 Hz). ³¹P{¹H} NMR (-70 °C, CD₂Cl₂): δ 21.3 (br d, *J*_{app} = 534 Hz), -3.7 (br d, *J*_{app} = 361 Hz). ¹³C{¹H} NMR (C₆D₆): δ 161.5 (t, *J* = 6 Hz), 132.1, 131.6, 122.2, 119.9, 117.0 (t, *J* = 20 Hz), 23.4 (m), 21.6, 21.0, 20.7 (t, *J* = 6 Hz), 20.2, 18.4. ³¹P{¹H} NMR (C₆D₆): δ 9.7 (d, *J*_{107-Ag-P} = 398 Hz, *J*_{109-Ag-P} = 449 Hz). Elem. Anal. Found (calcd) for C₂₆H₄₀P₂N₂Ag: C, 58.23 (58.22); H, 7.63 (7.52).

(PNP)Tl (9). To a stirring solution of TlOTf (251 mg, 0.71 mmol) in THF was slowly added **8** (309 mg, 0.71 mmol) in THF. The yellow-orange suspension was stirred for 20 min, and then the solvent was removed in vacuo. The remaining residue was dissolved in benzene and filtered. The orange filtrate was dried to give a thermally sensitive orange powder. This residue was extracted with diethyl ether and cooled to -36 °C overnight, yielding orange crystals of **9**. Yield: 370 mg (82%). ¹H NMR (C₆D₆): δ 7.30 (m, 2H, Ar-*H*), 7.04 (br s, 2H, Ar-*H*), 7.01 (s, 2H, Ar-*H*), 2.27 (s, 6H, Ar-CH₃), 2.24 (septet, 4H, CHMe₂), 1.08 (overlapping multiplets, 24H, CHMe₂). ²⁰⁵Tl NMR (25 °C, 289.286 MHz, C₆D₆): δ 3229 (t, *J*_{Tl-P} = 2434 Hz). ³¹P NMR (25 °C, 121.5 MHz, C₆D₆): δ 48.33 (d, *J*_{P-Tl} = 2385 Hz). ¹³C{¹H} NMR (25 °C, 125.69 MHz, C₆D₆): δ 161.8 (d, Ar), 134.3 (Ar), 132.3 (Ar), 123.7 (Ar), 120.9 (Ar), 120.0 (Ar), 25.0 (CHMe₂), 20.8 (ArMe), 19.9 (CHMe₂), 19.7 (CHMe₂). ¹³C NMR (25 °C, 125.69 MHz, C₆D₆): δ 161.8 (d, *J*_{C-P} = 31 Hz), 134.3 (d, *J*_{C-H} = 151 Hz, Ar), 132.3 (d, *J*_{C-H} = 152.4 Hz, Ar), 123.7 (s, Ar), 120.9 (d, *J*_{C-P} = 21 Hz, Ar), 119.4 (s, Ar), 25.0 (d, *J*_{C-H} = 129 Hz, CHMe₂), 20.8 (quartet, *J*_{C-H} = 125 Hz ArMe), 19.9 (quartet, *J*_{C-H} = 126 Hz, CHMe₂), 19.7 (quartet, *J*_{C-H} = 127 Hz, CHMe₂). Elem. Anal. Found (calcd) for C₂₆H₄₀NP₂Tl: C, 49.37 (49.33); H, 6.02 (6.37); N, 2.21 (2.21).

Synthesis of 10 from 9. To a J. Young NMR tube containing NiCl₂(THF)_{1.5} in THF was added a solution containing 1 equiv of **9** in THF. The formation of a white precipitate was observed immediately with a change in the color of the solution to green. Inspection by ³¹P and ¹H NMR spectroscopies revealed the formation of **10** and some **1**. On the basis of a *tert*-butylbenzene internal integration standard (5.0 μL), **11** was formed in 85% yield.

Synthesis of 11 with 9. To a J. Young NMR tube containing (COD)PdCl₂ (15.0 mg, 0.052 mmol) in C₆D₆ was added 1 equiv of **9** (33.2 mg, 0.052 mmol). The immediate formation of a white precipitate was accompanied by a change in the solution color from orange to red/purple. On the basis of the dioxane internal integration standard (5.0 μL), **11** was formed in >90% yield. Note that attempts to prepare **11** from **9** and anhydrous PdCl₂ resulted in decomposition mixtures after 24 h, presumably due to the decomposition of **9**.

Synthesis of 12 with 9. To a J. Young NMR tube containing (COD)PtCl₂ (11.0 mg, 0.029 mmol) in C₆D₆ was added 1 equiv of **9** (19.0 mg, 0.030 mmol) in C₆D₆. The resulting yellow solution was accompanied by the rapid precipitation of a white solid. On the basis of the dioxane internal integration standard (5.0 μL), **12** was formed in 94% yield.

Synthesis of 10 with 2. **2** (15.9 mg, 0.0298 mmol of Ag) was transferred to a screw-capped NMR tube in air and dissolved in C₆D₆ (used as received and stored outside the glovebox). Dioxane (2.5 μL) was added to the clear, bright-yellow solution as an internal integration standard. The solution rapidly became green upon the addition of (DME)NiCl₂ (8.2 mg, 0.0325 mmol). NMR analysis

(25) Muller, G.; Lachmann, J. *Z. Naturforsch., B: Anorg. Chem.* **1993**, *48*, 1544.

(26) Pangborn, A. B.; Giardello, M. A.; Grubbs, R. H.; Rosen, R. K.; Timmers, F. J. *Organometallics* **1996**, *15*, 1518.

(27) Woodhouse, M. E.; Lewis, F. D.; Marks, T. J. *J. Am. Chem. Soc.* **1982**, *104*, 5586.

(28) Kern, R. J. *J. Inorg. Nucl. Chem.* **1962**, *24*, 1105.

(29) Ward, L. G. L. *Inorg. Synth.* **1971**, *13*, 154.

(30) Drew, D.; Doyle, J. R. *Inorg. Synth.* **1990**, *28*, 346.

indicated formation of **10**, but the quantification was not possible because of the extensive overlap with the broad peaks of unidentified paramagnetic compounds also present in the solution.

Synthesis of 11 with 2. In a screw-capped NMR tube in air, **2** (15.7 mg, 0.0294 mmol of Ag) was dissolved in C₆D₆ (used as received and stored outside the glovebox) to form a clear, bright-yellow solution. Dioxane (2.5 μL) was added to the sample as an internal integration standard for ¹H NMR. Upon the addition of (COD)PdCl₂ (8.4 mg, 0.0295 mmol), an immediate color change was observed, with the solution rapidly becoming a cloudy red with a white precipitate. The solution was held at 70 °C for 2 h. **11** was observed in 90% yield (quantification by ¹H NMR based on the internal integration standard).

Synthesis of 12 with 2. In a screw-capped NMR tube in air, **2** (15.6 mg, 0.0292 mmol of Ag) was dissolved in C₆D₆ (used as received and stored outside the glovebox), generating a clear, bright-yellow solution. Dioxane (2.5 μL) was added to the sample to serve as an internal integration standard. (COD)PtCl₂ (13.3 mg, 0.0355 mmol) was added, resulting in the rapid formation of a cloudy yellow solution with a white precipitate. The solution was held for 2 h at 70 °C. **12** was observed in 90% yield (quantification by ¹H NMR based on the internal integration standard).

X-ray Data Collection, Solution, and Refinement for 2. All of the operations were performed on a Bruker-Nonius Kappa Apex2 diffractometer, using graphite-monochromated Mo Kα radiation. All of the diffractometer manipulations, including data collection, integration, scaling, and absorption corrections, were carried out using the Bruker Apex2 software.³¹ Preliminary cell constants were obtained from 3 sets of 12 frames. Data collection was carried out at 120 K, using a frame time of 10 s, and a detector distance of 60 mm. The optimized strategy used for data collection consisted of seven φ and ω scan sets, with 0.5° steps in φ or ω; a total of 1544 frames were collected. Final cell constants were obtained from the xyz centroids of 7174 reflections after integration.

From the lack of systematic absences, observed metric constants, and intensity statistics, space group *P* $\bar{1}$ was chosen initially; subsequent solution and refinement confirmed this to be the correct choice. The structure was solved using *SIR-92*³² and refined (full-matrix least squares, 586 parameters, 13 250 data) using the Oxford University *Crystals for Windows* program.³³ All of the non-H atoms were refined using anisotropic displacement parameters; H atoms were fixed at calculated geometric positions and allowed to ride on the corresponding C atoms. The final least-squares refinement converged to R1 = 0.0349 and wR2 = 0.0685 (*F*², all data).

X-ray Data Collection, Solution, and Refinement for 9. A preliminary set of cell constants was calculated from reflections obtained from 3 nearly orthogonal sets of 30 frames. The data collection was carried out using graphite-monochromated Mo Kα radiation with a frame time of 3 s and a detector distance of 5.0 cm. A randomly oriented region of a sphere in reciprocal space was surveyed. Four sections of 606 frames were collected with 0.30° steps in ω at different φ settings with the detector set at -43° in 2θ. Final cell constants were calculated from the xyz centroids of 1853 strong reflections from the actual data collection after integration (*SAINT 6.1*).³⁴

Intensity statistics and systematic absences suggested that the centrosymmetric space group *Pbca* and subsequent solution and refinement confirmed this choice. Data were corrected for absorption using the Bruker *SADABS* software.³⁵ The structure was solved using *SHELXS-97* and refined with *SHELXL-97*.³⁶ A direct-methods solution was calculated, which provided most of the non-H atoms from the *E* map. Full-matrix least-squares/difference Fourier cycles were performed, which located the remaining non-H atoms. All of the non-H atoms were refined with anisotropic displacement parameters. All of the H atoms were located in subsequent Fourier maps and included as isotropic contributors in the final cycles of refinement. The final full-matrix least-squares refinement converged to R1 = 0.0283 and wR2 = 0.062 (*F*², all data). The remaining electron density is located near the T1 site.

Acknowledgment. For financial support of this research, we thank Indiana University—Bloomington, Brandeis University, the donors of the Petroleum Research Fund, the Camille and Henry Dreyfus Foundation, the Alfred P. Sloan Foundation (research fellowships to D.J.M. and O.V.O.), the U.S. National Science Foundation (Grant CHE-0348941 and PECASE award to D.J.M., Grant CHE-0517798 to O.V.O., and Grant CHE-0521047 to B.M.F. (CCD diffractometer)). We thank Yanjun Zhu for assistance with the optimization of the synthesis of **2**. The authors at Indiana University wish to thank the Howard Hughes Medical Institute (HHMI) at Brandeis University for allowing them to borrow an NMR probe and Dr. John Tomaszewski at Indiana University.

Supporting Information Available: Crystallographic information in the form of CIF files and pictorial depictions of selected NMR spectra. This material is available free of charge via the Internet at <http://pubs.acs.org>.

IC0700598

(31) *Apex2*, version 2 user manual; Bruker Analytical X-ray Systems: Madison, WI, 2006; M86-E01078.

(32) Altomare, A.; Casciaro, G.; Giacovazzo, G.; Guagliardi, A.; Burla, M. C.; Polidori, G.; Camalli, M. *J. Appl. Crystallogr.* **1994**, *27*, 435.

(33) Betteridge, P. W.; Carruthers, J. R.; Cooper, R. I.; Prout, K.; Watkin, D. *J. Appl. Crystallogr.* **2003**, *36*, 1487.

(34) *SAINT 6.1*; Bruker Analytical X-Ray Systems: Madison, WI.

(35) An empirical correction for absorption anisotropy. Blessing, R. *Acta Crystallogr. A* **1995**, *A51*, 33.

(36) *SHELXTL-Plus*, version 5.10; Bruker Analytical X-Ray Systems: Madison, WI.